Design of waveguide amplifiers in high contrast erbium-doped $KY(WO_4)_2$ waveguides

Valentina Vaiti, Mustafa A. Sefunc, Sergio Vázquez-Córdova, Sonia M. García Blanco

Optical Sciences Group, MESA+ Institute for Nanotechnology, University of Twente, P.O. Box 217, 7500 AE Enschede, the Netherlands, e-mail: s.m.garciablanco@utwente.nl

On-chip amplifiers in high contrast erbium doped potassium double tungstate waveguides are theoretically studied. The high confinement of the electromagnetic field in these waveguides permits large erbium concentrations to be inverted with relatively low pump power. The total net gain is calculated as a function of pump power. In order to increase the coupling of pump and signal light into the high contrast waveguide amplifiers, adiabatic input tapers are investigated.

Introduction

Erbium ion doped potassium double tungstate [Er^{3+}:$KY(WO_4)_2$] high contrast waveguide amplifiers are expected to achieve high gain per unit length with small pump power, leading to short, efficient amplifiers suitable for integration with passive photonic platforms [1]. In this paper, the amplifier model utilized in the modelling of high contrast erbium ion doped potassium tungstate waveguide amplifiers is presented. The total net gain is calculated as a function of incident pump power. In order to increase the coupling of pump and signal fields into the high contrast waveguide amplifiers, adiabatic input tapers have been designed. A comparison of the theoretical results of the total net gain of waveguide amplifiers with input tapers optimized for three different in-coupling configurations (i.e., input fiber with MFD = 4 µm, input fiber with MFD = 10 µm, free space) with the total net gain of a straight waveguide was carried out in order to demonstrate the efficiency of the designed structure.

Amplifier model

In the optimization of a rare-earth ion doped waveguide amplifiers, different design parameters need to be considered, including the geometrical waveguide cross-section that provides monomode operation at both pump and signal wavelengths, the pump and the signal wavelengths, the rare-earth ion dopant concentration and the launched pump power range. In this work, the waveguide cross-section depicted in Fig. 1 (a) was considered. It consists of a 2 µm by 2.4 µm ridge of height 1.5 µm made in Er^{3+}:$KY(WO_4)_2$ with 0.5 µm thick Er^{3+}:$KY(WO_4)_2$ under-ridge. The Er^{3+}:$KY(WO_4)_2$ ridge waveguide is bonded to a SiO_2 on Si substrate by means of a 3 µm thick NOA81 adhesive. Air is considered as cladding material in this work. The high refractive index contrast geometry allows for high confinement in the straight and taper sections of the waveguide. 10 at. % Er^{3+} doping was utilized in this study.

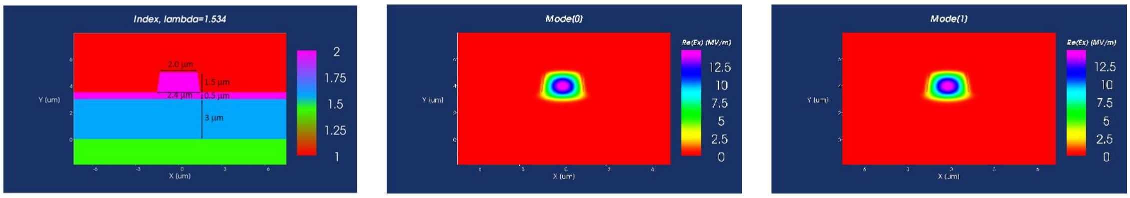

(a) (b) (c)

Fig. 1 (a) Waveguide amplifier cross-section. The materials from the substrate are: SiO_2 (green), NOA81 adhesive (blue), Er^{3+}:$KY(WO_4)_2$ (KYW) (pink) and air (red); (b) Pump mode profile distribution at 1487 nm and (c) Signal mode profile distribution at 1532 nm.

The *PhoeniX FieldDesigner Software* [2] was utilized to calculate the mode-field distributions of the pump and signal fields using a finite differences (FD) algorithm. Special attention has been given to the discretization of the structure. A non-uniform grid was utilized. Both x-axis and y-axis were divided into 129 sections with non-uniform space distribution, more concentrated in the doped region amplifier. In Fig.1, the signal-mode profile distribution at the wavelength of 1532 nm (b) and the pump-mode profile distribution at wavelength of 1487 nm (c) are displayed. A simplified 3-level rate equation model for the Er^{3+} was utilized (Fig. 2).

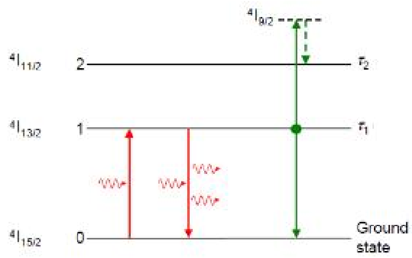

Fig. 2 Schematic of the energy levels of Er^{3+}.

When using a pump wavelength of 1487 nm, the Er^{3+} ion is directly pumped into the $^4I_{13/2}$ level. Stimulated emission on the pump transition $^4I_{15/2} \leftrightarrow {}^4I_{13/2}$ at 1480 nm plays a more significant role than on the pump transition $^4I_{15/2} \leftrightarrow {}^4I_{11/2}$ at 980 nm, due to the significantly longer lifetime and, consequently, larger population density in the $^4I_{13/2}$ level compared to the $^4I_{11/2}$ level. In the three-level energy model, the stimulated absorption, spontaneous emission and stimulated emission caused by the interaction of light with matter are considered. In addition, the first energy transfer up-conversion (ETU) process, which can have an important effect on the amplifier performance, has also been considered. The first ETU process involves the energy transfer between two ions in the $^4I_{13/2}$ level, promoting one ion to an upper level ($^4I_{9/2}$) and the de-excitation of the other to the ground state ($^4I_{15/2}$). This process decreases the population of the amplifier $^4I_{13/2}$ state. The rate equations utilized in this work have been described in detail in [3]. The values utilized in our simulations are summarized in Table 1.

Waveguide amplifiers with input tapers

In order to increase the coupling of pump and signal into the high contrast waveguide amplifiers, the used of adiabatic input tapers (i.e., with angle 0.5 deg) was investigated. Three different launching scenarios were considered. On the first one, an input fiber with mode-field diameter (MFD) of 10 µm was considered. In the second scenario, a small core fiber was considered, with MFD = 4 µm. In the last scenario, coupling from free space was considered. The initial width of the input taper was calculated so that the mode overlap between the MFD of the input fiber (or the spot size obtained in free space) and the fundamental mode of a ridge waveguide with the initial width of the input taper was maximized. Once the initial width of the input taper was calculated, the linear taper was then sliced in a sufficiently large number of slices. Both the signal and pump mode profiles were then calculated for each of the slices and the rate equations were solved to determine the populations of each of the Er^{3+} levels, the total net gain in that slice and the absorbed pump power. Such calculation is then carried out for each of the following slices, considering the new values of pump and signal power. Since the taper is adiabatic, propagation losses due to the taper are neglected.

Table 1. Parameters and Values Applied to the Gain Simulations.

Parameters	Pump	Signal
Wavelength [nm]	1487	1534
Abs. Cross Section [m^3/sec]	$1.75*10^{-24}$	$2.5*10^{-24}$
Emis. Cross Section [m^3/sec]	$0.7*10^{-24}$	$2.5*10^{-24}$
Background Loss [dB/m]	3.2236	3.2236
Incident Power	5-50 [mW]	1 [uW]

Lifetime	
Level 1 [sec]	$120*10^{-6}$
Level 2 [sec]	$3.1*10^{-3}$
Energy Transfer Up-conversion [cm^(3) / sec]	
ETU ~ $5*10^{-19}$	
Erbium concentration	
10%	

Table 2. Parameters and values applied to the input adiabatic taper simulation.

Adiabatic Taper θ= 0.5		
MFD	**10**	**4**
Winp [um]	6	5
Wout [um]	2	2
Taper Length [mm]	0,458	0,343

Gaussian Overlap		
	Taper	**Straight**
MFD = 10	20%	10%
MFD = 4	68%	48%

In Table 2, the parameters used in the taper calculations are presented. The total length of the amplifier was 7 mm. The total net gain obtained with the taper was compared with the net gain of a straight waveguide 2 µm wide. In Fig. 3 the calculated total internal gain for different pump power values in the three input coupling scenarios is displayed. When using an input fiber with MFD = 10 µm [Fig. 3 (a)], adding an adiabatic input taper permits reaching better performance for lower pump powers than in a straight waveguide amplifier. The mode overlap between the input fiber with MFD = 10 µm and a 2 µm wide ridge waveguide is only of 20%. For low pump powers, the structure with the taper achieves higher inversion than the straight waveguide. It also reaches full inversion more rapidly. Only for high pump power values (200 mW), both structures achieve the same results in both cases. When using a small core fiber with MFD = 4 µm [Fig. 3 (b)], the advantage of using the input adiabatic taper is much lower. The reason is the higher coupling efficiency from this fiber to the 2 µm wide ridge waveguide, which only improves slightly by the introduction of the taper.

A model M-60x objective lens (see Table 3) was considered for free space coupling, since this lens has similar numerical aperture to the waveguide of this study. Using this lens, a MFD of 1.73 µm can be achieved, which provides an optimum value of overlap with an input ridge waveguide 2 µm wide. Therefore, an input taper is not required. The total net gain for incident pump powers ranging from 5 to 100 mW is shown in Fig.3 (c).

Table 3. Parameters and Values Applied to calculate the MFD achieved with a lens (free space case)

Model	Magnification	Numerical Aperture (NA)	Focal Length [mm]	Working Distance [mm]	Clear Aperture [mm]
M-60X	60x	0.85	2.9	0.3	4.5

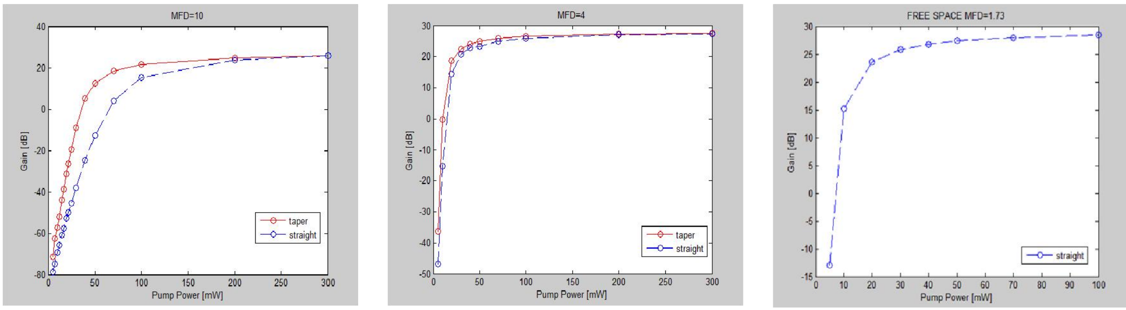

(a) (b) (c)

Fig. 3 Calculated internal net gain at different pump power values for a 7 mm long Er^{3+} doped waveguide amplifier: simulations with (red curves) and without (blue curve) input adiabatic taper: (a) Input fiber MFD = 10 µm; (b) Input fiber MFD = 4 µm; and (c) Coupling from free space (input beam diameter 1.73 µm).

Conclusions

In this work, we demonstrated how the high confinement of the electromagnetic field permits large erbium concentration to be inverted with relatively low pump power. The total internal net gain was the key factor in the selection of the implementation of an adiabatic linear taper or a straight waveguide. We demonstrated how the choice depends on the lens type and on the mode field diameter selected. With MFD = 10 µm we reached a good performance and a good gain value whit the use of a taper; in the MFD = 4 µm and free space scenario, an implementation of the designed structure is not useful and a straight waveguide is advised.

Future works may involve the structure of the amplifier model, in particular the dimensions and the structure of the doped channel waveguide, always taking into account the percentage of erbium concentration.

References

[1] M.A. Sefunc, F.B. Segerink, S.M. García-Blanco, "High index contrast potassium double tungstate waveguides towards efficient rare-earth ion amplification on-chip," Proc. SPIE 9365, 93650P (2015).

[2] www.phoenixbv.nl

[3] J. Bradley, "*Al_2O^3:Er^{3+} as a gain platform for integrated optics*", University of Twente Thesis, 2009.